

Mechanisms generating spatial variability in Ross Sea biogeochemical fields

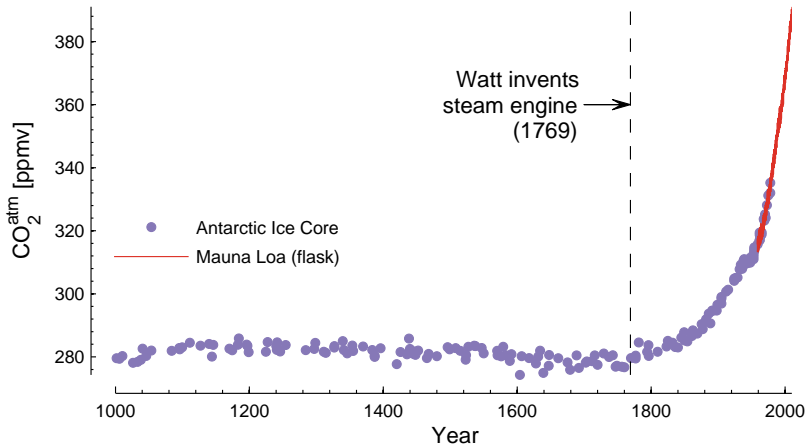
Matthew C. Long

National Center for Atmospheric Research
Climate and Global Dynamics Division

15 November 2010

Global carbon cycle

Atmospheric CO₂



Global carbon cycle



Atmosphere

Anthropogenic CO₂

4.1 Pg C a⁻¹
45%

Natural CO₂ reservoir

600 Pg C



Land biosphere

3.0 Pg C a⁻¹
29%

2300 Pg C
 $\sim 4 \times$ Atm



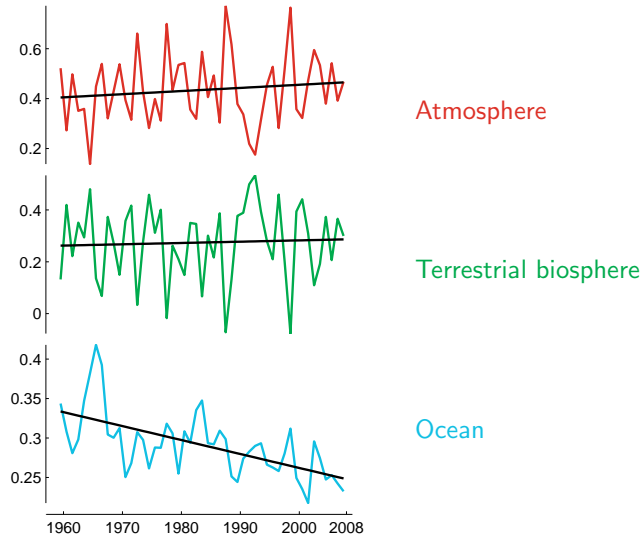
Ocean

2.3 Pg C a⁻¹
26%
for 2000–2008

38,000 Pg C
 $\sim 60 \times$ Atm
 $\sim 16 \times$ Land

Efficiency of natural CO₂ sinks

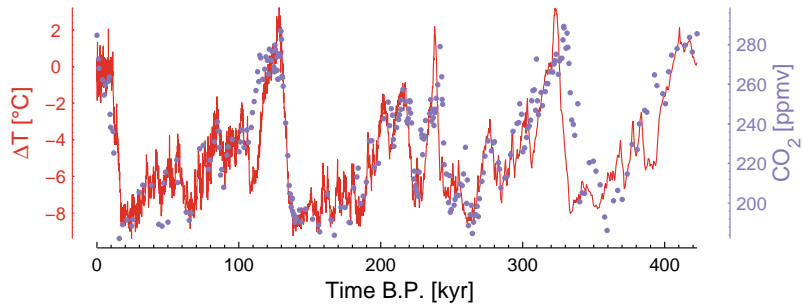
CO₂ uptake, fraction of emissions



Canadell et al. 2007, PNAS

Global carbon cycle

Glacial/interglacial cycles



Petit et al. 1999

Outline

1. Motivation

Global carbon cycle: Nutrient utilization in Southern Ocean deepwater formation regions controls ocean-atmosphere partitioning of CO₂.

2. Introduction to the Ross Sea

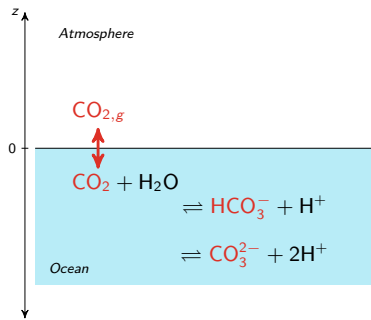
An important deepwater formation region, characterized by strong seasonality in surface forcing.

3. Mechanisms generating variability in biogeochemical fields

Spring: Ekman restratification at ocean fronts;

Summer: Ice melt, stirring, and algal community composition.

Carbon in seawater



Dissolved inorganic carbon:

$$DIC \equiv [\text{CO}_2] + [\text{HCO}_3^-] + [\text{CO}_3^{2-}]$$

where [] denote concentrations in solution.

HCO_3^- → bicarbonate

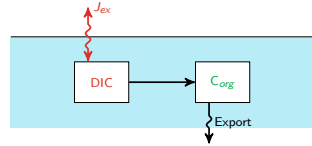
CO_3^{2-} → carbonate

Solubility pump

$$[\text{CO}_2]_{sat} = f(T, S)$$

$$\boxed{\frac{\partial \text{DIC}}{\partial z}} \uparrow \implies p\text{CO}_2^{\text{atm}} \downarrow$$

Biological pump

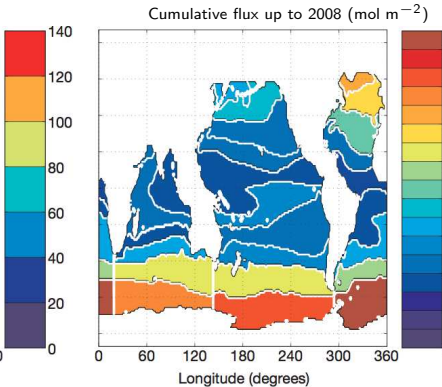
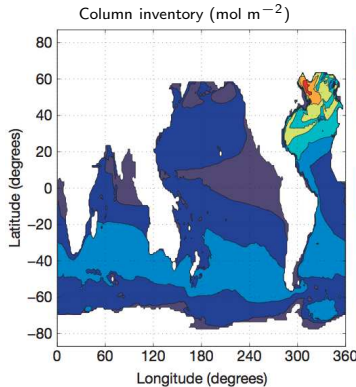


$$J_{ex} = (1 - A_{ice})k\gamma (p\text{CO}_2^{\text{atm}} - p\text{CO}_2^{\text{sw}})$$

Importance of the Southern Ocean

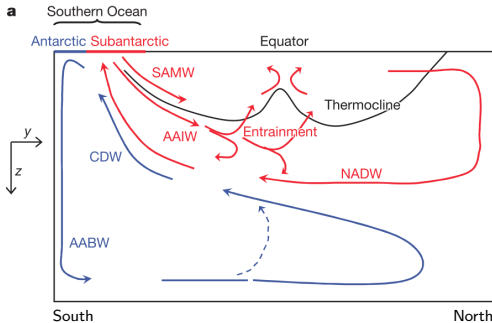
Anthropogenic CO₂ in the ocean

~ 40% entered through the Southern Ocean



based on tracer time distributions
Khatiwala et al. 2009

Southern Ocean: meridional circulation



SAMW: Subantarctic Mode Water
AAIW: Antarctic Intermediate Water
NADW: North Atlantic Deep Water
CDW: Circumpolar Deep Water
AABW: Antarctic Bottom Water

Marinov et al. 2006

Divergence poleward of the Polar Front brings deepwater to the surface.

Upper cell: Subduction forms northward-flowing Antarctic Intermediate Water and Subantarctic Mode Water.

Lower cell: Antarctic Bottom Water is formed along the continental margin.

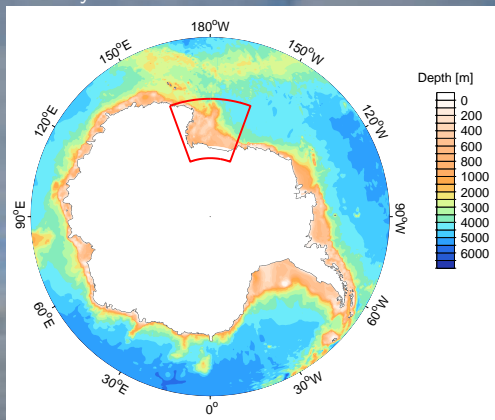
CORSACS cruises

Controls on Ross Sea Algal Community Structure



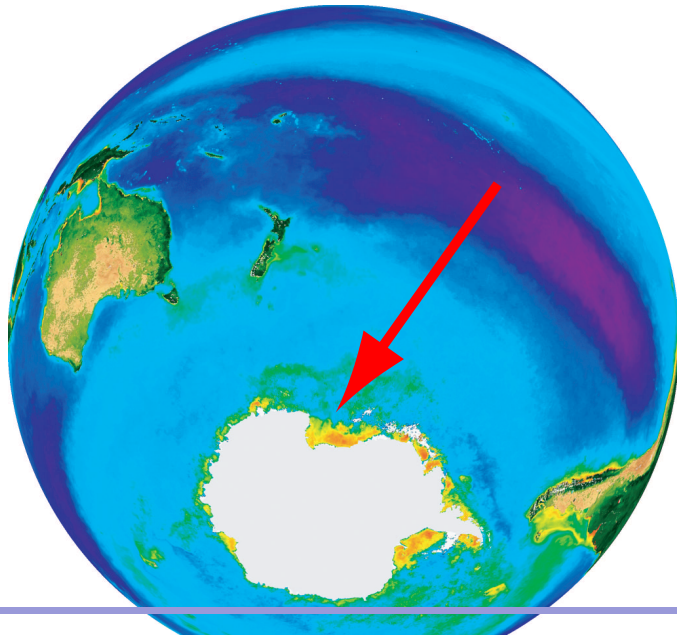
CORSACS cruises

Controls on Ross Sea Algal Community Structure

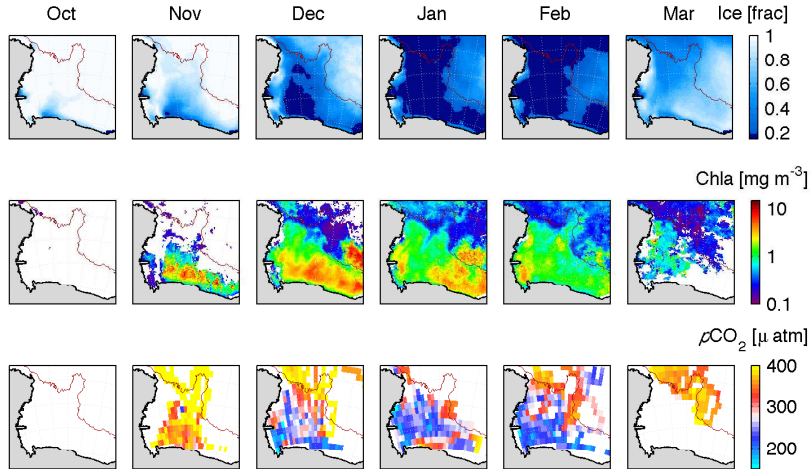




The most productive region in Southern Ocean



Annual polynya formation

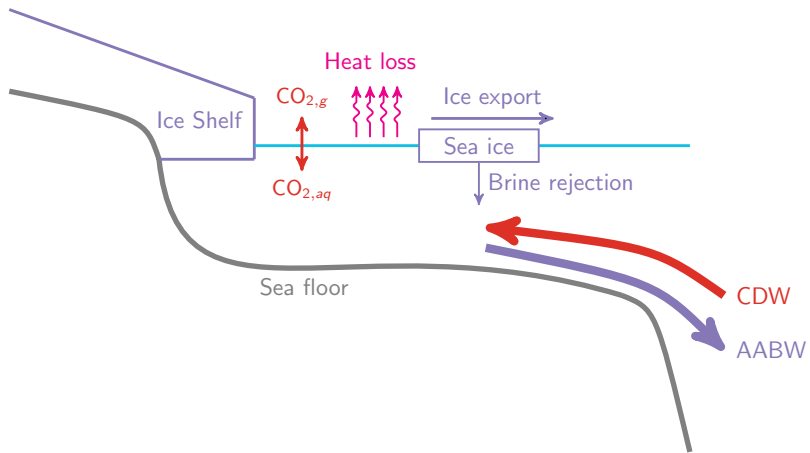


Top: SSM/I ice, fraction of ice free time (1995–2006)

Middle: SeaWiFS chlorophyll a(1997–2006)

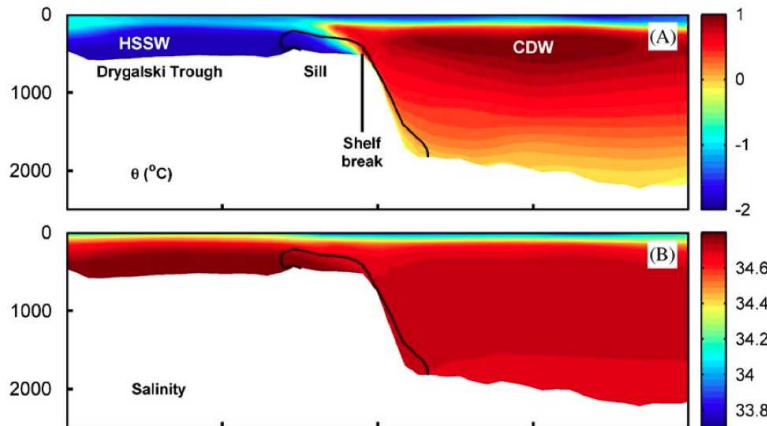
Bottom: $p\text{CO}_2^{\text{sw}}$ climatology from all *R/V N. B. Palmer* data (1995–2006)

Antarctic continental shelves



Deepwater formation

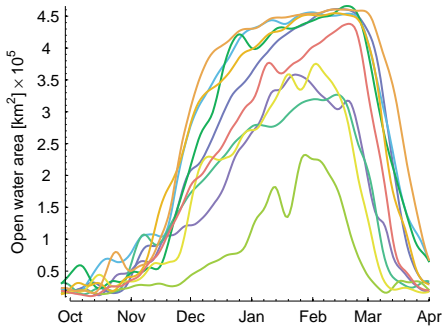
Ross Sea temperature and salinity



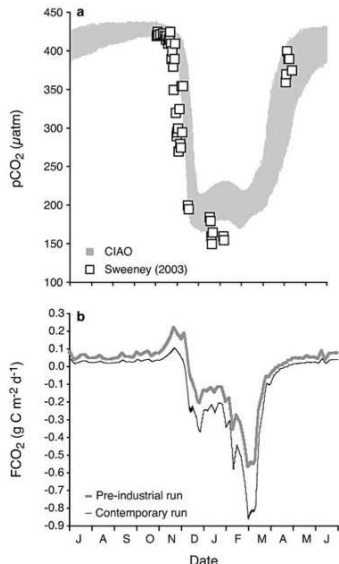
Padman et al. 2009

CO_2 sink: biogeochemical modeling results

Polynya formation (1996–2006)



- ▶ As ice clears, phytoplankton bloom reduces $p\text{CO}_2^{\text{sw}}$;
- ▶ Sea ice limits winter outgassing;
- ▶ Net CO_2 sink: 13 Tg C yr^{-1} ;
 $\sim 5\%$ of entire Southern Ocean.

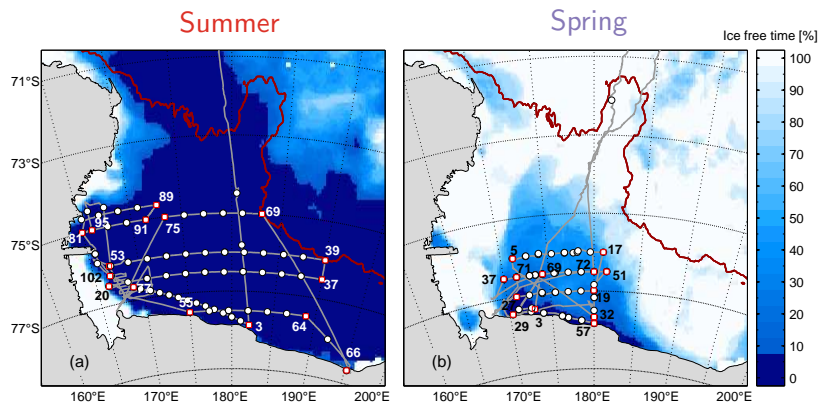


Arrigo et al. 2008

Research question

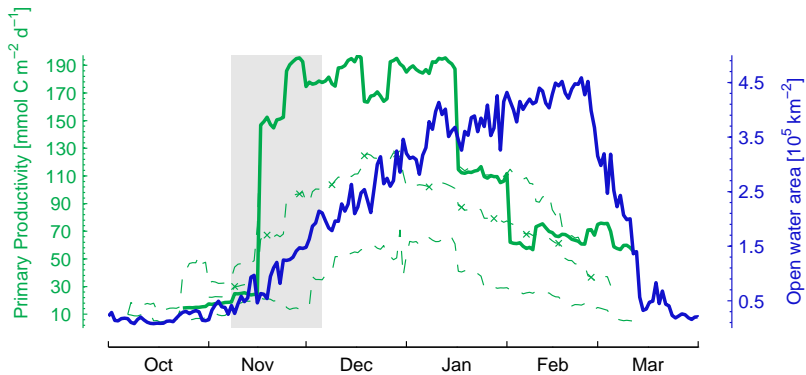
What mechanisms control the spatial and temporal variability of primary productivity and biogeochemical fluxes on the Ross Sea continental shelf?

CORSACS stations



Spring cruise: 2006–2007

Satellite primary productivity and open water area:

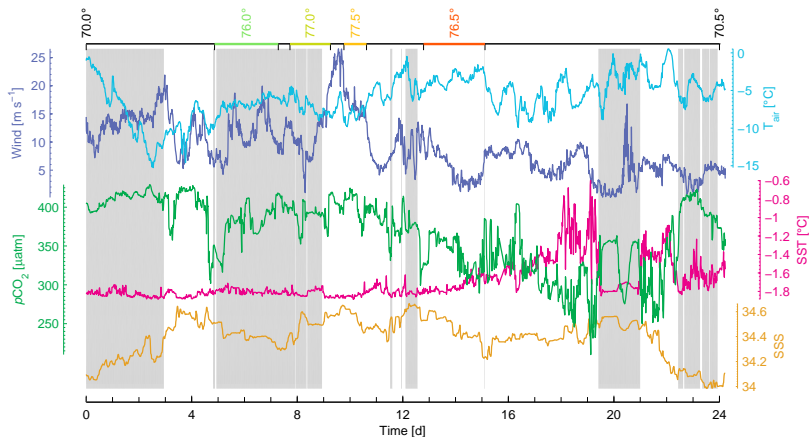


Bloom is taking off, temporal rates of change are high!

Long et al. 2010

Spring $p\text{CO}_2^{\text{sw}}$ decline

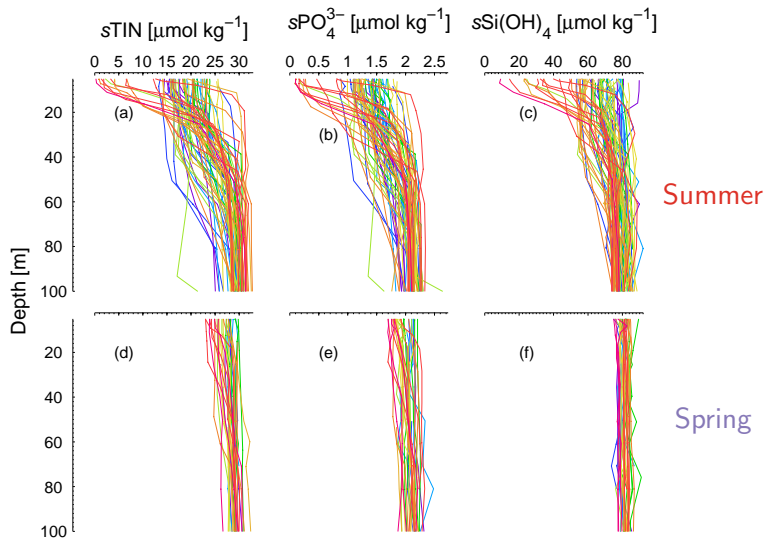
mid-November–early-December



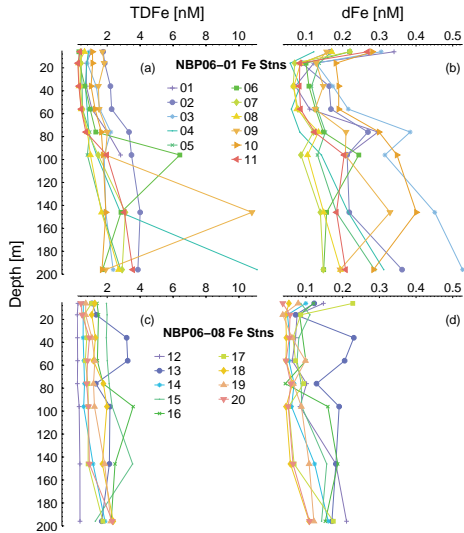
Background: gray = ice, white = open water.

Long et al. submitted

Nutrient replete



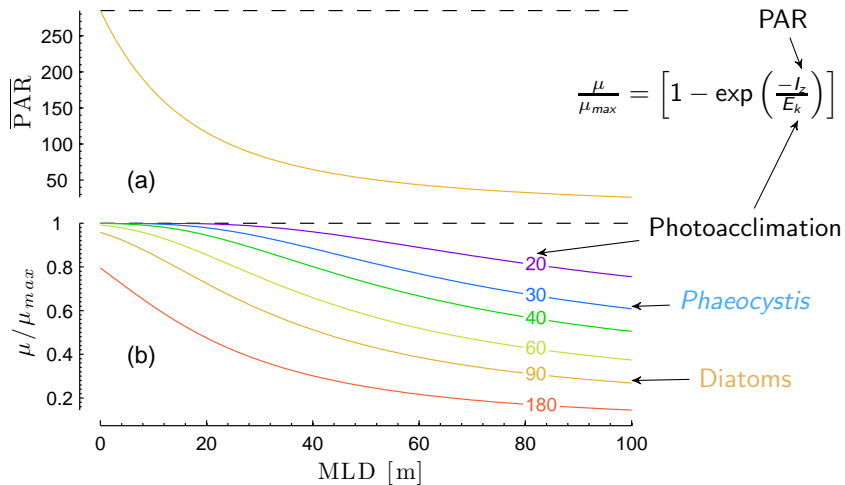
Low iron variability (& low iron)



Summer

Spring

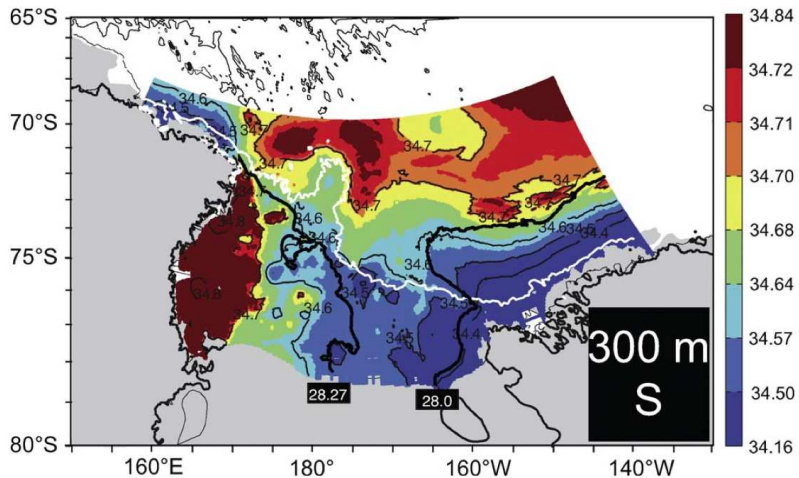
Restratification can alleviate light limitation



PAR = photosynthetically available radiation

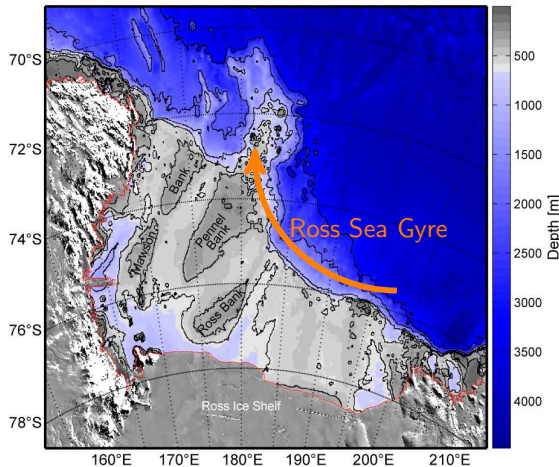
Climatological hydrography

Zonal salinity gradient



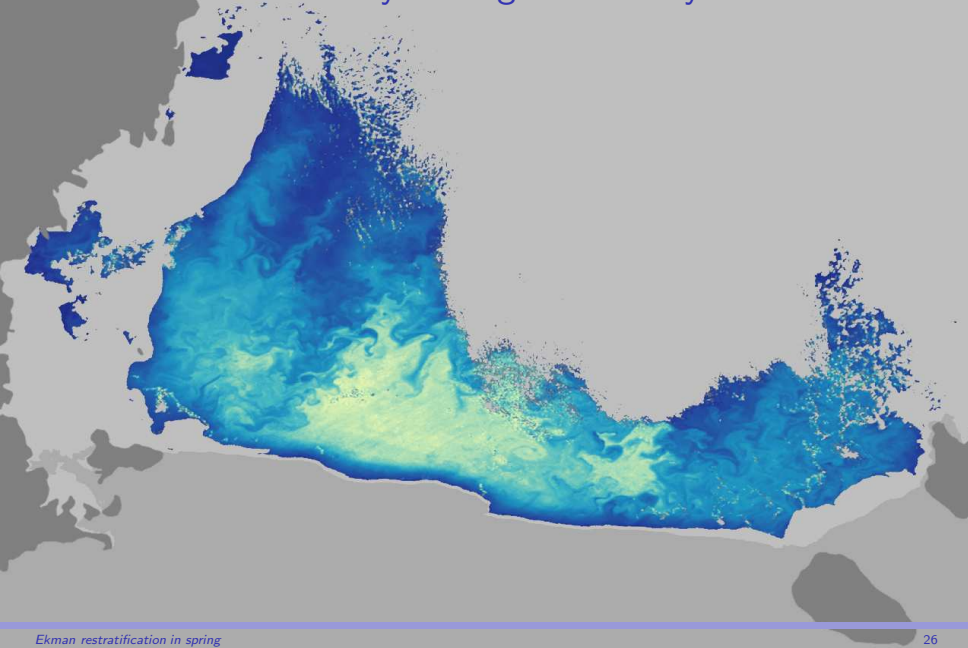
Orsi & Wiederwohl 2009

Shelf topography interacts with mean flow



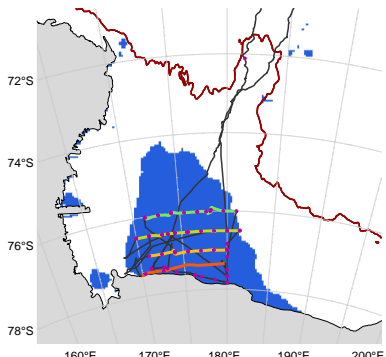
- ▶ Regional flow drives confluence of different water masses
- ▶ Flow is largely barotropic, thus shaped by topography

Submesoscale variability in biogeochemistry



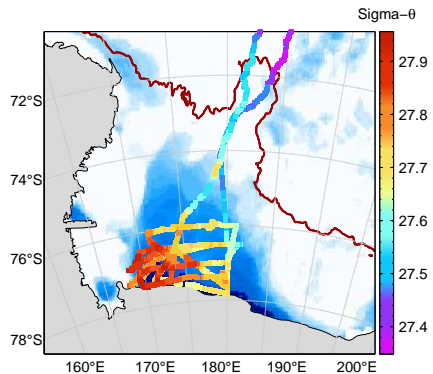
Observations of spring bloom

Cruise track and ice



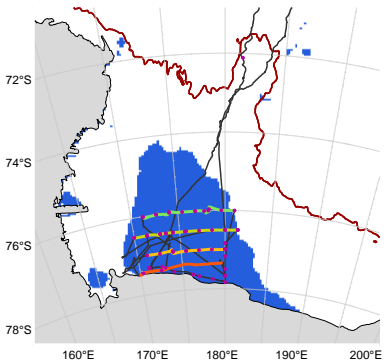
Long et al. submitted

Zonal density gradient

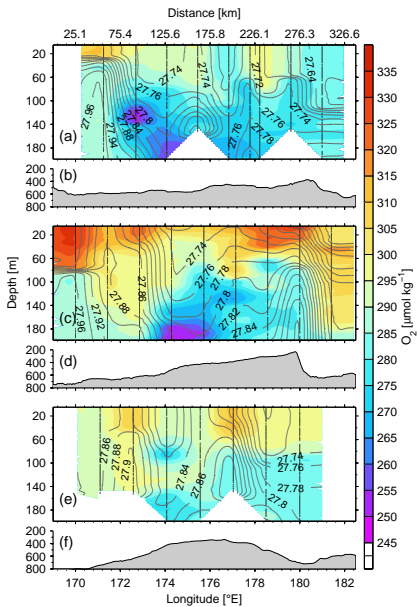


Observations of spring bloom

Cruise track and ice



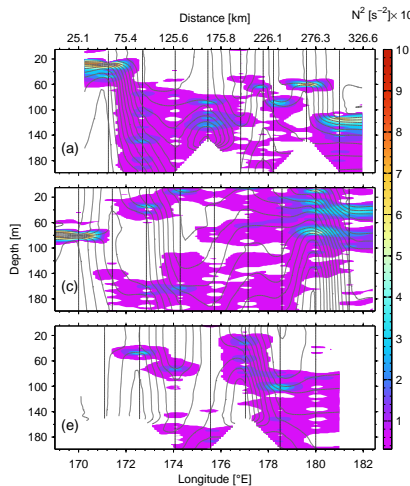
Elevated oxygen concentrations
found to the west of fronts. } →



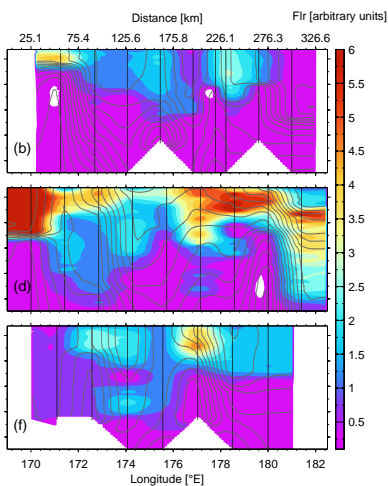
Long et al. submitted

Observations of spring bloom

Buoyancy frequency



Chlorophyll a Fluorescence

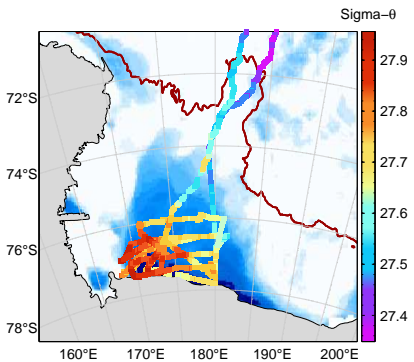


Enhanced stratification and elevated biomass associated with fronts.

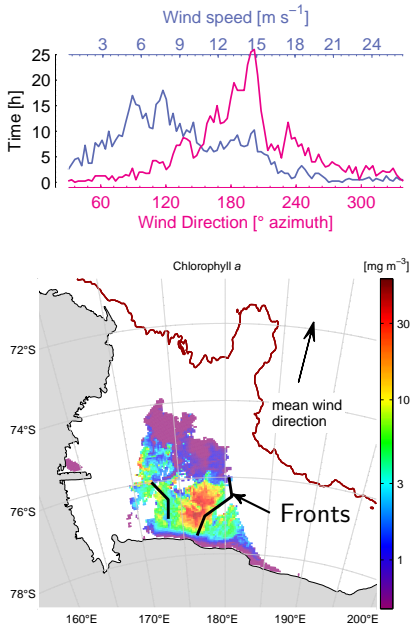
$$N^2 = -(g/\rho)d\rho/dz$$

Observations of spring bloom

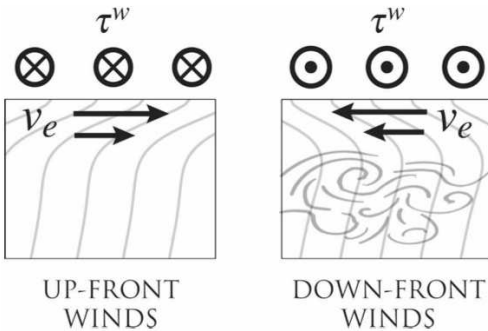
Zonal density gradient



Predominantly southerly winds:
tendency for Ekman transport to
advection light water over dense.



Hypothesis: Ekman restratification

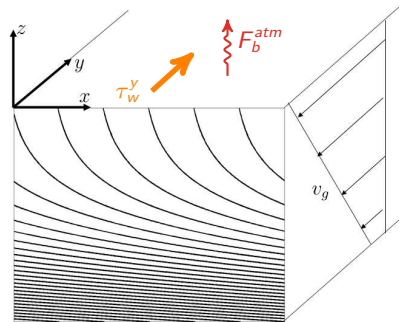


(Northern Hemisphere example)

Thomas & Ferrari 2008

Numerical Experiments

- ▶ Modified version of ROMS, using biogeochemical model of *Fennel et al.* [2006].
- ▶ Vertical mixing parameterized using KPP [*Large et al.* 1994].
- ▶ Density structure and biogeochemical fields initialized using spring cruise data.



EXP 1: 1D surface buoyancy fluxes only;

EXP 2: 2D uniform lateral buoyancy gradient ($3 \times 10^{-8} \text{ s}^{-2}$); and

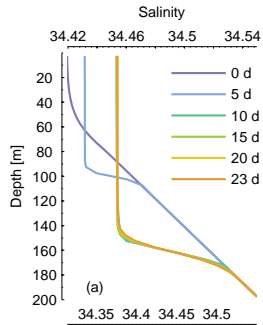
EXP 3: 2D variable lateral buoyancy gradient initialized using

$$S_i = s(z) + \frac{\partial \bar{s}}{\partial x} x + \sum_{n=1}^3 a_n \sin \left(\frac{2n\pi x}{L} + \phi_n \right),$$

fit to salinity observations along 76°30'S.

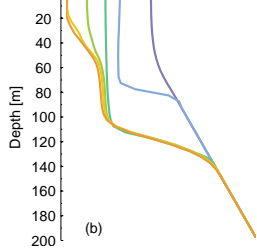
Salinity evolution in 1D and 2D experiments

EXP1 (1D)



- ▶ **1D case:** mixed layer deepens continually, entrainment increases salinity and density;

EXP2 (2D)



- ▶ **2D case:** Ekman advection of buoyancy limits mixed layer depth; pycnostads are formed, capping relic mixed layers.

Defining the Ekman buoyancy flux (EBF)

Buoyancy equation:

$$\frac{\partial b}{\partial t} = -\nabla \cdot (\mathbf{u}b + \mathbf{F}^b)$$

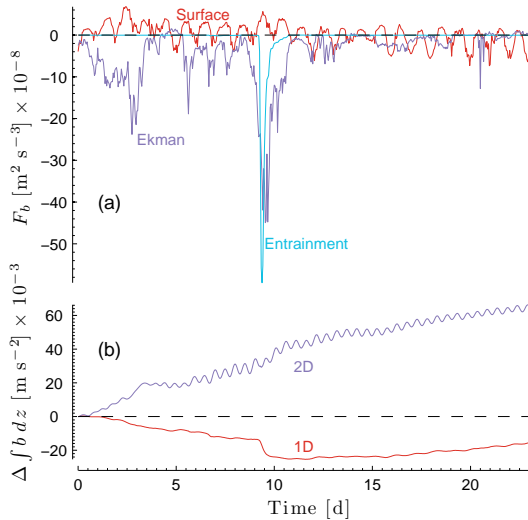
Integrated over depth h (2D experiments):

$$\frac{\partial}{\partial t} \int_{-h}^0 \bar{b} dz = -\bar{F}_b^{atm} + \bar{F}_b^{ent} - \int_{-h}^0 \bar{u} \frac{\partial \bar{b}}{\partial x} dz$$

Ekman buoyancy flux ($h > \delta_{ek}$):

$$\text{EBF} = \int_{-h}^0 \bar{u} \frac{\partial \bar{b}}{\partial x} dz = \mathbf{M}_e \cdot \nabla_h b_s$$

Ekman advection provides stabilizing buoyancy flux

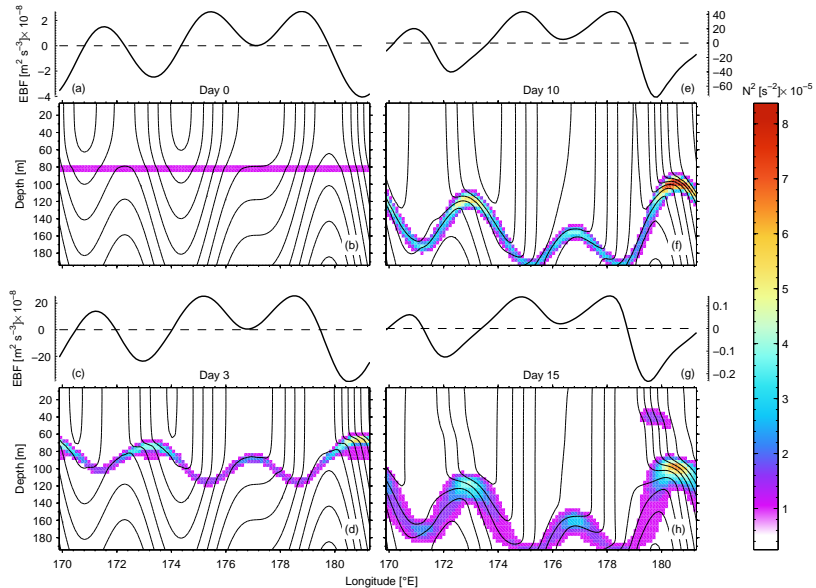


Positive surface flux indicates cooling (i.e. $F_b^{atm} \uparrow$).

During initial high winds, EBF dominates over destabilizing F_b^{atm} .

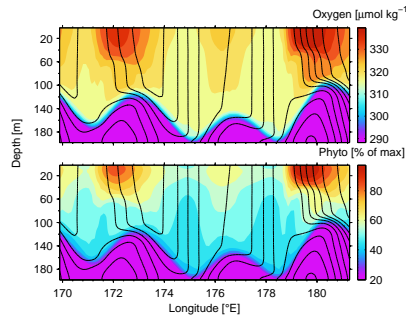
Except in strongest winds, the EBF is greater than buoyancy losses associate with entrainment at the base of the mixed layer (F_b^{ent}).

Deep and shallow mixed layers in close proximity

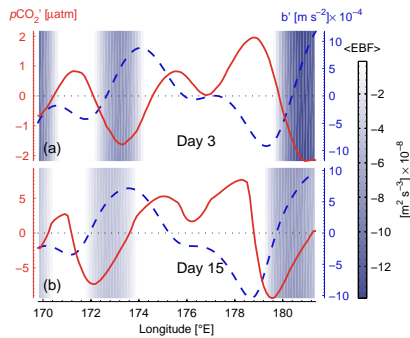


Mixed layer variations are reflected in biogeochemical fields

O₂ and phytoplankton biomass



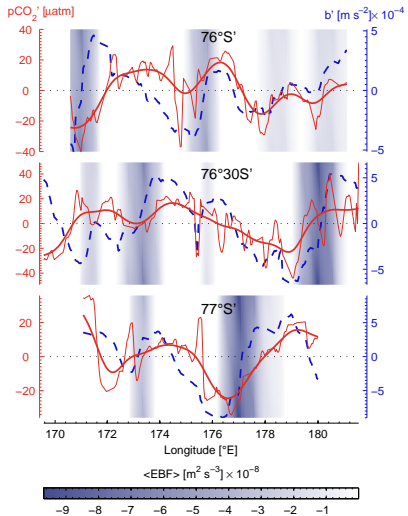
$p\text{CO}_2^{\text{sw}}$, $\partial b/\partial x$, and EBF



- ▶ Ekman restratification enhances primary productivity;
- ▶ Biomass and oxygen accumulation, as well as CO₂ drawdown are enhanced where EBF < 0.

Divining the signature of the EBF

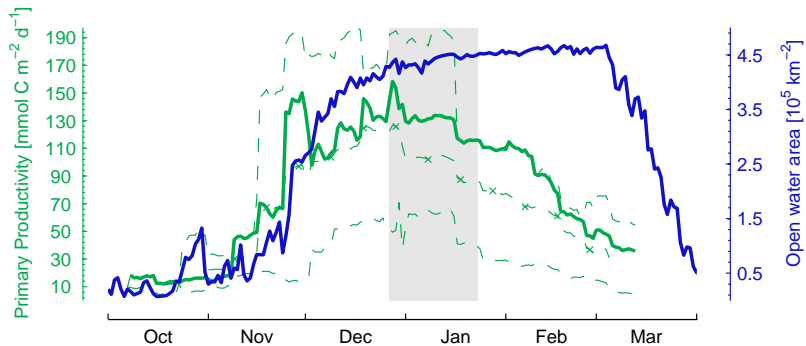
$p\text{CO}_2^{\text{sw}}$ observations (zonal anomalies)



- ▶ $p\text{CO}_2^{\text{sw}}$ is correlated with buoyancy field and the EBF on about 10 km scales;
- ▶ Phasing of relationship complicated by space-time convolution inherent in observations.

Summer cruise: 2005–2006

Satellite primary productivity and open water area:



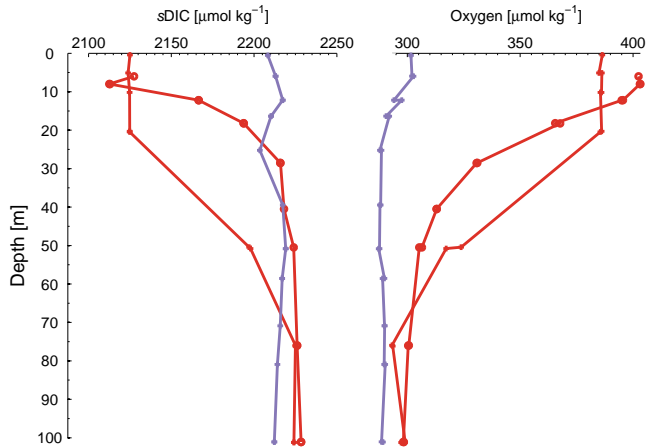
After bloom peak, substantial portion of seasonal NCP already occurred, rates of change are low.

Long et al. accepted, JGR

Deep convection homogenizes spring water column

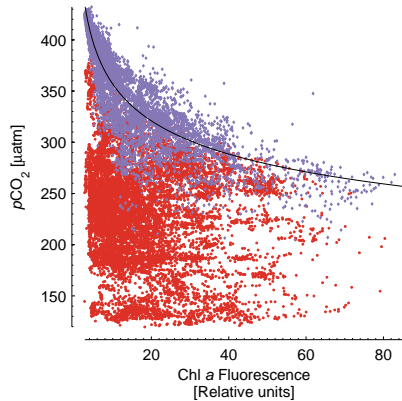
Variance is constructed *de novo* each summer.

Typical profiles:



Rate processes decouple from geochemical tracers

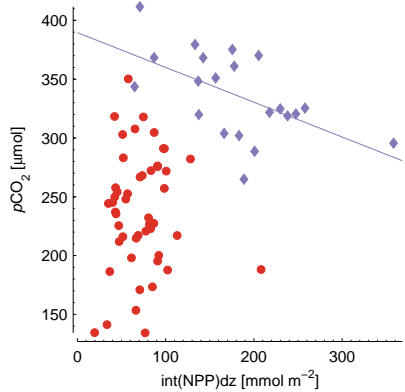
$p\text{CO}_2^{\text{sw}}$ v. chlorophyll a



Summer/Spring

Long et al. accepted, JGR

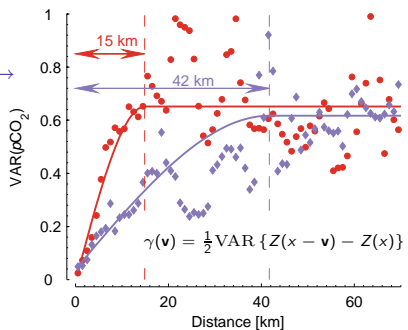
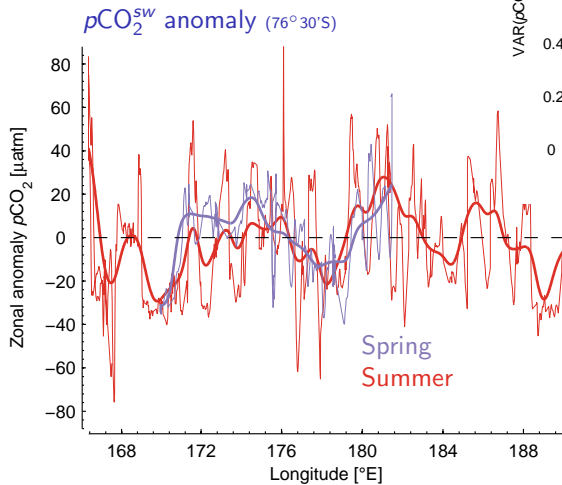
$p\text{CO}_2^{\text{sw}}$ v. NPP



NPP = net primary production
determined by ^{14}C incubation

Variance propagates downscale

Structure function →



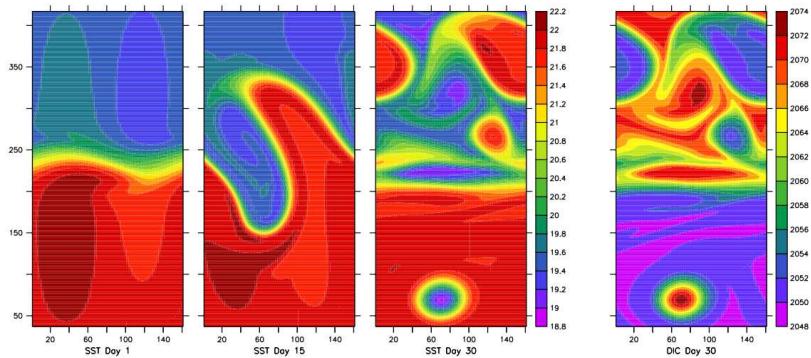
Front is in the same place!

Lateral gradients intensify due to time-integrated biological production;

Stirring enhances short-length scale variability in summer.

Variance propagates downscale

Evolution of an unstable baroclinic front

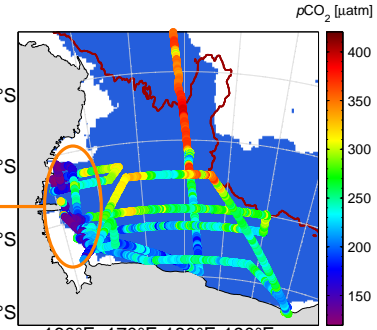
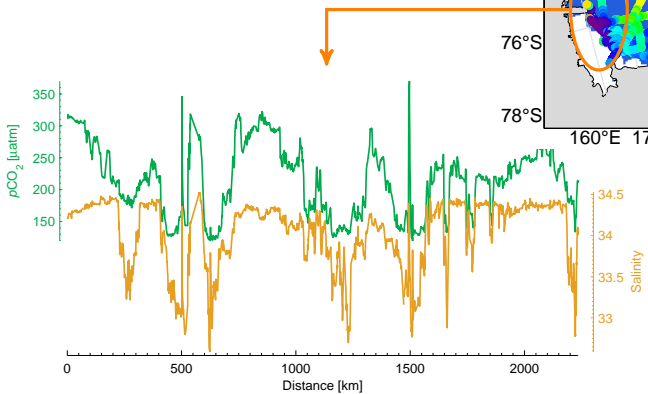


Initial DIC distribution: $\text{DIC}_0 = f(T)$

Mahadevan et al. 2004

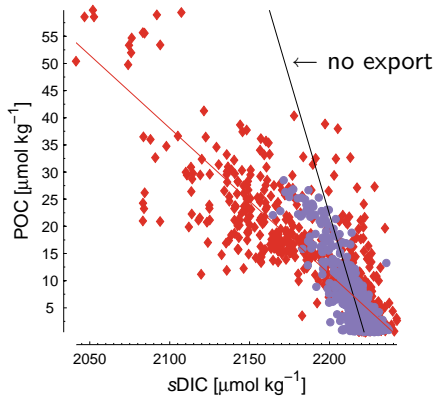
Locally intense $p\text{CO}_2^{\text{sw}}$ drawdown due to ice-melt

As the mixed layer depth is reduced, NPP is integrated over a smaller volume.



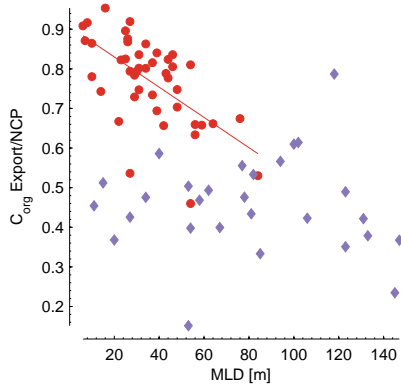
Shallow mixed layers export a higher percentage of C_{org}

C_{org} v. sDIC

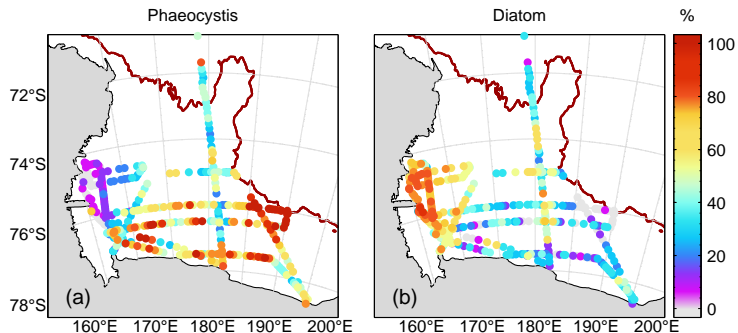


Summer/Spring

Export fraction v. mixed layer depth



Community composition aligns with mixed layer depth

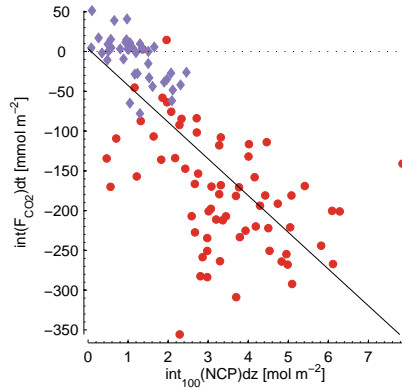


	Export ratio	$r_{C:P}$	$r_{C:N}$	ϵ_p [%]
--	--------------	-----------	-----------	------------------

<i>Phaeocystis</i>	0.50 ± 0.08	117 ± 7	6.7 ± 0.3	-20.8 ± 0.1
Diatom	0.78 ± 0.11	73 ± 3	5.9 ± 0.3	-16.2 ± 0.3

Air-sea exchange is proportional to net production

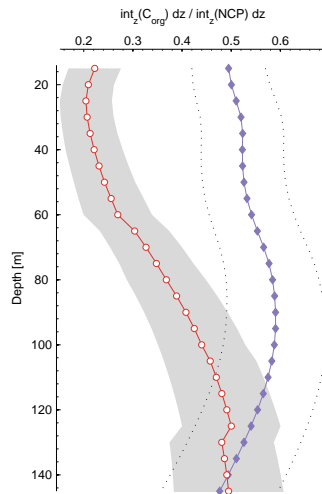
Air-sea CO₂ flux v. NCP



$$\int_{\text{Oct}}^{\text{Jan}} F_{\text{CO}_2} dt = f(\text{NCP})$$

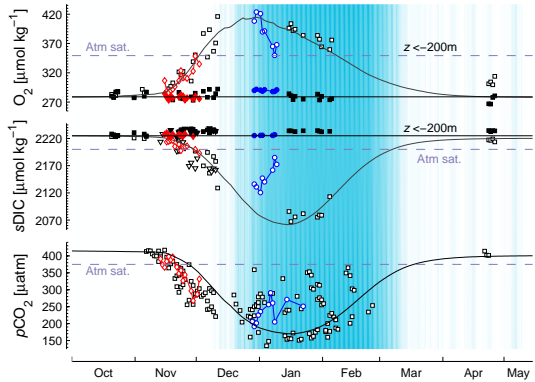
NCP = net community production
 = NPP — Respiration

C_{org} left in the water column



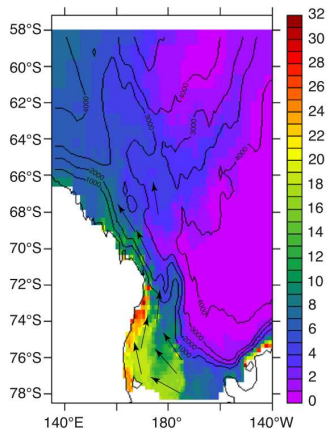
Understanding the fate of carbon on the Ross Sea shelf

Observations and box model



Overflow/entrainment

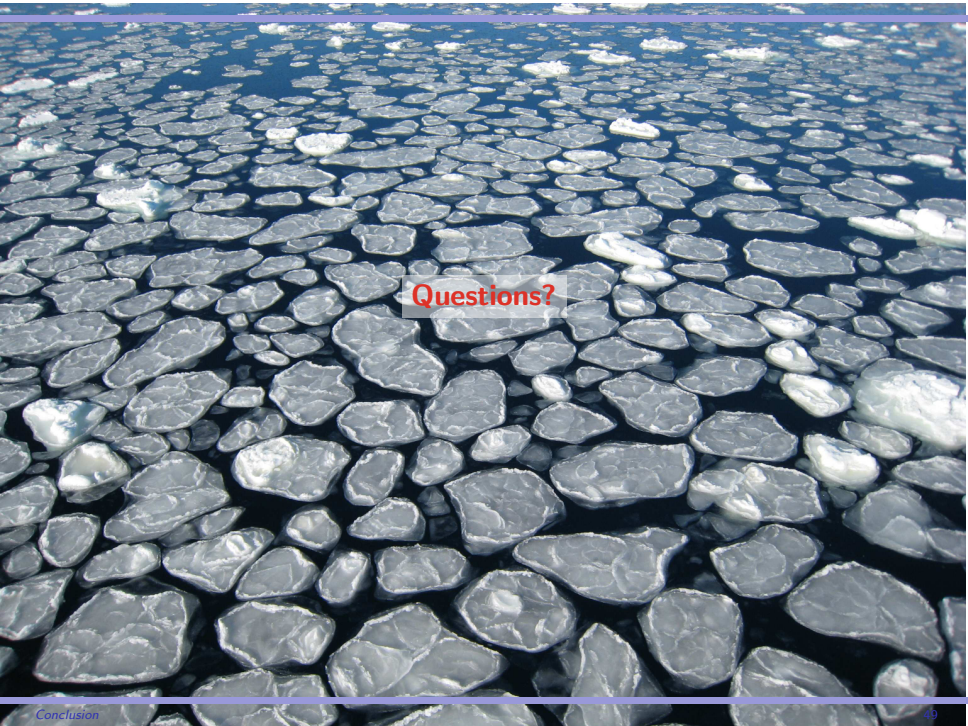
Anthropogenic TCO_2 ($\mu\text{mol kg}^{-1}$)



Arrigo et al. 2008

Summary

- ▶ Ekman restratification plays an important role triggering the spring bloom, contributing $\sim 20\%$ of annual production (2006–2007);
- ▶ Solar heating and ice-melt derived freshwater fluxes drive restratification later in the season;
- ▶ Fronts linked to bathymetry explain the location of recurring blooms; interannual variability in wind direction can modulate the magnitude of seasonal primary production;
- ▶ Accurately representing the processes affecting stratification, rates of NPP, and air-sea exchange is important to resolving the global ocean carbon cycle;
- ▶ In the future, biogeochemical fluxes are likely to change due to different physical regimes *and* shifts in algal community composition.



A wide-angle photograph showing a dense field of broken sea ice. The ice pieces are various sizes and shapes, ranging from small floes to larger, more irregular blocks. They are set against a dark, reflective background of deep blue water. The lighting creates highlights on the edges of the ice floes, emphasizing their texture and the overall pattern they create.

Questions?